BASIC SCIENCE

Nanomedicine: Nanotechnology, Biology, and Medicine
17 (2019) 308 – 318

nanomedicine
Nanotechnology, Biology, and Medicine

Original Article

nanomedjournal.com

Non-viral vectors based on cationic niosomes and minicircle DNA technology enhance gene delivery efficiency for biomedical applications in retinal disorders

Idoia Gallego, PhD[a,b,1], Ilia Villate-Beitia, MSc[a,c,1], Gema Martínez-Navarrete, PhD[c,d], Margarita Menéndez, PhD[e,f], Tania López-Méndez, MSc[a,c], Cristina Soto-Sánchez, PhD[c,d], Jon Zárate, PhD[a,c], Gustavo Puras, PhD[a,c,*], Eduardo Fernández, PhD[c,d], José Luis Pedraz, PhD[a,c,*]

[a]*NanoBioCel Group, University of the Basque Country (UPV/EHU), Vitoria-Gasteiz, Spain*
[b]*Ikerbasque, Basque Foundation for Science, Bilbao, Spain*
[c]*Biomedical Research Networking Center in Bioengineering, Biomaterials and Nanomedicine (CIBER-BBN), Spain*
[d]*Neuroprothesis and Neuroengineering Research Group, Miguel Hernández University, Elche, Spain*
[e]*Rocasolano Physical Chemistry Institute, Superior Council of Scientific Investigations (IQFR-CSIC), Madrid, Spain*
[f]*Biomedical Research Networking Center in Respiratory Diseases (CIBERES), Spain*

Revised 9 November 2018

Abstract

Low transfection efficiency is a major challenge to overcome in non-viral approaches to reach clinical practice. Our aim was to explore new strategies to achieve more efficient non-viral gene therapies for clinical applications and in particular, for retinal diseases. Cationic niosomes and three GFP-encoding genetic materials consisting on minicircle (2.3 kb), its parental plasmid (3.5 kb) and a larger plasmid (5.5 kb) were combined to form nioplexes. Once fully physicochemically characterized, *in vitro* experiments in ARPE-19 retina epithelial cells showed that transfection efficiency of minicircle nioplexes doubled that of plasmids ones, maintaining good cell viability in all cases. Transfections in retinal primary cells and injections of nioplexes in rat retinas confirmed the higher capacity of cationic niosomes vectoring minicircle to deliver the genetic material into retina cells. Therefore, nioplexes based on cationic niosomes vectoring minicircle DNA represent a potential tool for the treatment of inherited retinal diseases.

Key words: Non-viral vector; Niosomes; Minicircle; Transfection; Gene therapy; Retina

Abbreviations: MC, Minicircle; pGFP, plasmid with green fluorescent protein; pEGFP, plasmid with enhanced green fluorescent protein; PDI, polydispersity index; TEM, transmission electron microscopy; SDS, sodium dodecyl sulfate; ITC, isothermal titration calorimetry; IV, intravitreal; SR, subretinal

Conflicts of interest: The authors declare no personal or professional conflicts of interest.

Funding source declaration: This work was supported by the Basque Country Government (Department of Education, University and Research, pre-doctoral grant PRE_2016_2_0302 and Consolidated Groups, IT907-16), the Ikerbasque Foundation for Science from the Basque Country, the Spanish Grant MAT 2015-69976-C3-1, SAF2013-42347-R, and by the Research Chair "Bidons Egara".

Acknowledgments: Authors wish to thank the intellectual and technical assistance from the ICTS "NANBIOSIS", more specifically the Drug Formulation Unit (U10) of the CIBER in Bioengineering, Biomaterials and Nanomedicine (CIBER-BBN) at the University of the Basque Country (UPV/EHU). Technical and human support provided by SGIker (UPV/EHU) and European funding (ERDF and ESF) is gratefully acknowledged, as well as to Dr. José Manuel Andreu (CIB-CSIC) for supplying the access to PEAQ-ITC equipment.

*Corresponding authors at: Laboratory of Pharmacy and Pharmaceutical Technology, School of Pharmacy, University of the Basque Country (UPV/EHU), Paseo de la Universidad 7, 01006, Vitoria-Gasteiz, Spain.

E-mail addresses: gustavo.puras@ehu.eus (G. Puras), joseluis.pedraz@ehu.es (J.L. Pedraz).

[1] Idoia Gallego and Ilia Villate-Beitia contributed equally to this work.

https://doi.org/10.1016/j.nano.2018.12.018
1549-9634/

The pathogenesis of several blinding retinal disorders such as retinitis pigmentosa, Leber's congenital amaurosis, macular dystrophies and age-related degeneration of the macula among others, has a genetic background.[1,2] Currently, there is no effective treatment for these kind of disorders and, to date, gene therapy strategies seem to be one of the most promising field of research [3,4]. Non-viral gene delivery approaches have key safety advantages over viral vectors and their use in clinical trials has gained importance since 2004; meanwhile the viral vectors ones have significantly decreased [5] due to their risk of oncogenesis, immunogenicity, mutagenicity and even the persistence of viral vectors in the brain after intravitreal injection [6–8]. Particularly, cationic lipids are actually among the most commonly used non-viral vectors [5,9].

Niosomes are drug delivery systems able to bind genetic material, forming complexes known as nioplexes, with the ability to protect the DNA from enzymatic digestion and to introduce it into the cell with controlled release kinetics. Furthermore, they present low toxicity due to their biocompatibility and biodegradability, are osmotically active, chemically stable formulations, and are easy to handle [10,11], establishing as a better alternative than the common liposomes. Niosomes are composed by cationic lipids to form complexes with the negatively charged DNA by electrostatic interactions [12], helper lipids to promote the physico-chemical and biological properties of the complex [13,14], and non-ionic surfactants to enhance the stability [15]. Recently, their capacity to transfect *in vivo* brain and retinal cells in rats has been reported[16–19]. Even though the low toxicity of nioplexes preserves cell viability when transfected, the major challenge to reach the clinical practice is the limited transfection efficiency [20]. Therefore, more research efforts are required for the successful implementation of niosomes as optimal gene delivery carriers.

Currently, minicircle (MC) DNA technology offers a potential solution to the reduced transfection efficiency translational barrier for gene therapy. MCs are small circular DNA vectors with no antibiotic resistant genes or bacterial backbone sequences, which make them superior to regular plasmids. MC-DNA has a reduced size compared with conventional plasmid DNA with the same expression cassette and the content of unmethylated CpG dinucleotides is considerably reduced. Thus, their use results in sustained transgene expression due to lower activation of nuclear transgene silencing mechanisms, and reduced immunogenic responses *in vivo* [21–26].

Our goal is to provide as far as we are concerned, the first evidence that niosome based non-viral vectors combined with the MC technology is an effective technique for future clinical applications in the retinal gene therapy field. We employed DST20 formulation comprised of cationic lipid 1,2-di-O-octadecenyl-3-trimethylammonium propane (DOTMA), the helper lipid Squalene and the non-ionic surfactant polysorbate Tween 20 [17–19]. The resulting niosomes were combined with three different DNA materials consisting on MC-GFP of 2257 bp, pGFP of 3487 bp and pEGFP of 5541 bp, to form the corresponding nioplexes. Niosomes and nioplexes were characterized in terms of particle size, polydispersity index (PDI), zeta potential, morphology and stability. The capacity of niosomes to protect and release these DNA materials as well as the binding interactions between cationic niosomes and DNAs at molecular level was also analyzed. *In vitro* experiments were performed to evaluate both the efficiency and cell viability of transfection over time and at different temperatures with the three DNA materials complexed to DST20 niosomes in human ARPE-19 retinal pigment epithelium cells. Additionally, the transfection capacity of these nioplexes was assessed by *ex vivo* experiments in embrionary rat retinal primary cells and by *in vivo* administration of nioplexes to rat eyes *via* intravitreal (IV) and subretinal (SR) injections.

Methods

Production of cationic niosomes

Niosomes based on cationic lipid DOTMA (Avanti Polar Lipids, Inc., Alabama, USA), helper lipid squalene (Sigma-Aldrich, Madrid, Spain) and the polysorbate Tween 20 (Sigma-Aldrich, Madrid, Spain) were prepared using the o/w emulsification technique to a molar ratio of 2 mM cationic lipid/ 8 mM helper lipid/ 4 mM tensioactive. The emulsion was obtained by sonication (Branson Sonifier 250, Danbury) for 30 s at 50 W. The dichloromethane organic solvent was removed from the emulsion by evaporation under magnetic agitation for 3 h at room temperature, obtaining the niosome DST20 solution.

DNA material: plasmids and minicircle technology

The 5541 bp pCMS-EGFP plasmid (Clontech laboratories, Inc., USA) (Figure 1), here named as pEGFP 5.5 kb, was propagated in *Escherichia coli* DH5-α and purified using the Qiagen endotoxin-free plasmid purification Maxi-prep kit (Qiagen, California, USA) according to manufacturer's instructions. The concentration of the purified pDNA was quantified by measuring the absorbance at 260 nm in a SimpliNano™ spectrophotometer device (GE Healthcare, Buckinghamshire, UK).

The 3487 bp pCMV-GFP plasmid (PlasmidFactory, Bielefeld, Germany) was employed as the parental plasmid of the 2257 bp MC.CMV-GFP minicircle (PlasmidFactory, Bielefeld, Germany) (Figure 1), which was devoid of any selection markers such as antibiotic resistance genes and bacterial origin of replication (ori). Here we abbreviated as pGFP 3.5 kb for the parental plasmid and MC-GFP for the resulting minicircle.

Preparation of nioplexes

The nioplexes were prepared by mixing an appropriate volume of a stock solution of either MC-GFP (1 mg/ml), pGFP 3.5 kb (1 mg/ml) or pEGFP 5.5 kb (0.5 mg/ml), with a volume of the niosome DST20 suspension (1 mg DOTMA/ml) to obtain a DOTMA/DNA ratio (w/w) of 2/1. The mixture was incubated for 30 min at room temperature before use to enhance electrostatic interactions between the cationic lipid and the negatively charged DNAs.

Physicochemical characterization of niosomes and nioplexes

Z-average particle size and PDI were determined by dynamic light scattering, and zeta potential was measured by laser Doppler velocimetry in a Zetasizer Nano ZS (Malvern

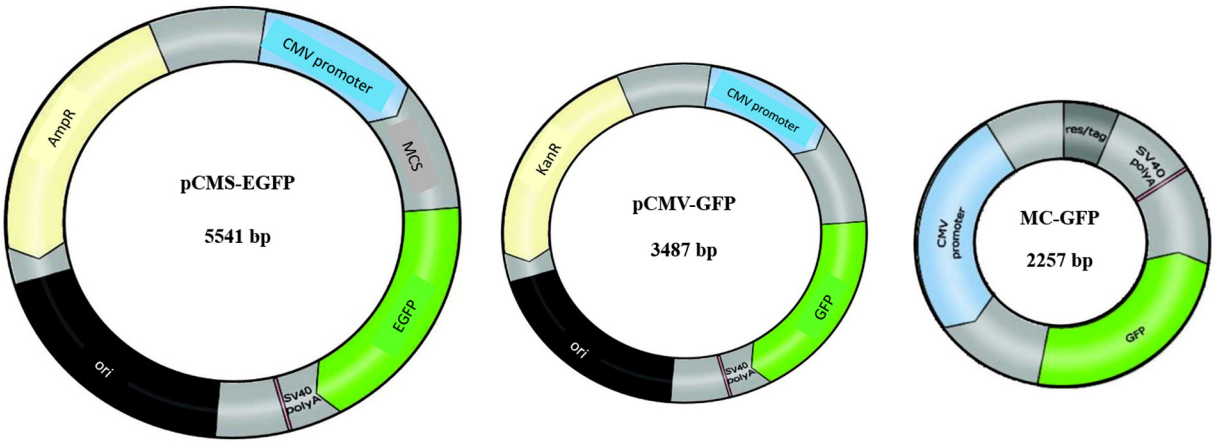

Figure 1. DNA material composition.**(A)** pEGFP 5.5 kb, **(B)** pGFP 3.5 kb, **(C)** MC-GFP 2.3 kb. MC: minicircle; GFP: green fluorescent protein; EGFP: enhanced green fluorescent protein; pCMS: plasmid containing Cytomegalovirus promoter, Multiple cloning site and SV40 promoter; pCMV: cytomegalovirus promoter plasmid; bp: base pairs.

Instruments, UK) previous resuspension of the samples into NaCl 1 mM solution. The particle size, reported as hydrodynamic diameter, was achieved by cumulative analysis. The Smoluchowski approximation supported the calculation of the zeta potential from the electrophoretic mobility. All measurements were carried out in triplicate.

The morphology of niosomes was assessed by transmission electron microscopy (TEM) as previously described [17]. The capacity of niosomes to protect and release the genetic material from enzymatic digestion was analyzed by a gel retardation assay as previously described [27]. Naked DNA was used as control at each condition, being the amount of DNA per well 100 ng in all cases.

Niosome-DNA interactions for nioplexes formation were analyzed by isothermal titration calorimetry (ITC) using a MicroCal PEAQ-ITC microcalorimeter (Malvern Instruments, UK). The assay was executed at 25 °C by stepwise injection of DST20 (0.25 mg/ml DOTMA) into the reaction cell loaded with an aqueous solution of the DNA material (0.0166 mg/ml). Typically, 1 × 0.4 μl injection followed by 13 × 3 μl injections was carried out automatically under 750 rpm stirring. In selected experiments, a second set of injections followed the first one after refilling the injection pipette with the same DST20 solution. The heat contributed by niosome dilution was measured in separate runs and subtracted from the total heat produced following each injection prior to the data analysis. The full set of experiments achieved at a given condition was carried out with the same dilution of niosomes in order to minimize errors.

Stability assays

DST20 niosomes were evaluated for stability at day 0 and after their storage for 30 days at 4 °C and 25 °C. Stability test consisted of the analysis of niosomes and nioplexes at day 0 and after the aforementioned storage in terms of particle size, PDI, zeta potential, TEM, gel retardation assay and ITC, as previously mentioned. Additionally, biological stability of niosomes in terms of transfection efficiency and cell viability was assessed *in vitro* at the aforementioned storage conditions.

Cell culture and in vitro transfection assays

Human retinal pigment epithelium cells ARPE-19 (ATCC, CRL-2302™) were transfected with nioplexes at the day 0 of the DST20 niosomes preparation and after the storage of niosomes for 30 days at 4 °C and 25 °C. Cells were seeded without antibiotics in the medium in 24 well plates at 12×10^4 cells per well and incubated overnight to achieve 70% of confluence at the time of transfection. The formation of DST20:DNA complexes composed of DST20 niosomes and 1.25 μg DNA of either MC-GFP, pGFP 3.5 kb or pEGFP 5.5 kb at 2/1 (w/w) DOTMA/DNA ratio, was left to occur through electrostatic interactions for 30 min at room temperature. Medium was removed and cells were washed with serum-free OptiMEM solution (Gibco, California, USA). Next, cells were exposed to nioplexes diluted in serum-free OptiMEM solution for 4 h at 37 °C for transfection. After incubation, the transfection medium was removed and fresh medium was added to the cells.

Transfection efficiency was analyzed qualitatively and quantitatively by fluorescence microscopy imaging (EclipseTE2000-S, Nikon) and by flow cytometry (FACSCalibur, BD Biosciences), respectively, 48 h after the exposure to nioplexes. To analyze cell viability, cells were stained with ethidium homodimer-1 (Life Technologies, Paisley, UK) prior to flow cytometry. A minimum of 10,000 events was collected and analyzed for each sample. Lipofectamine™ 2000 (Invitrogen, California, USA) was used as positive control, and corresponding lipoplexes were prepared according to the manufacturer's protocol. Non-transfected cells but incubated with OptiMEM for 4 h were employed as negative control. Each condition was performed in triplicate.

Animal model

Adult male Sprague-Dawley rats were used as experimental animal model. All experimental procedures were carried out in accordance with the Spanish and European Union regulations for the use of animals in scientific research and the Association for Research in Vision and Ophthalmology (ARVO) statement for

the use of animals in ophthalmic and vision research. Procedures were supervised by the Miguel Hernández University Standing Committee for Animal Use in Laboratory.

Transfection assays in rat primary retinal cell culture and immunocytochemistry

Embrionary rat retinal primary cells were extracted from E17.5 rat embryos from n = 4 Sprague Dawley rats. Transfection assays with nioplexes were performed at the day 0 of the DST20 niosomes preparation. Cells were seeded on poly-D-lysine-coated coverslips in 12 well plates at 2×10^5 cells per well. The composition of DST20:DNA nioplexes and the transfection conditions were the same as the previously mentioned ones for *in vitro* assays. Lipofectamine™ 2000 was used as positive control.

Transfection efficiency was analyzed qualitatively 96 h after the exposure to nioplexes by immunocytochemistry. Cellular phenotypes were assessed using specific antibody markers. For that, coverslips were incubated overnight with rabbit polyclonal anti-rabbit microtubule associated protein-2 (MAP2) (1:400 dilution; Millipore) as neuronal marker and with secondary antibody donkey anti-rabbit IgG Alexa Fluor 555 (1:200 dilution; Thermo Fisher Scientific), previous wash with PBS. Cell nuclei were stained with Hoechst 33342 (Thermo Fisher Scientific). Fluorescence analysis was performed with a Zeiss AxioObserver Z1 (Carl Zeiss) microscope equipped with an ApoTome system and different fluorescence filters.

Intravitreal and subretinal administration of nioplexes

The injection solution consisted of 4 μl of nioplexes suspension containing 100 ng of either the plasmids or MC. Nioplexes were injected in the left eyes of adult male Sprague-Dawley rats (6-7 weeks old and 150-200 g body weight) intravitreally (n = 3) or subretinally (n = 3) under an operating microscope (Zeiss OPMI® pico; Carl Zeiss Meditec GmbH, Jena, Germany) with the aid of a Hamilton microsyringe (Hamilton Co., Reno, NV), as previously described [17]. The untreated right eyes served as negative control. Lipofectamine™ 2000 was used as positive control of gene delivery.

Evaluation of GFP expression in rat retina

GFP expression was evaluated qualitatively 96 h after the injection of nioplexes in whole-mount and sagittal sections of the retina, as previously described [17]. Images of GFP signal were acquired using a Leica TCS SPE spectral confocal microscope (Laica Microsystems GmbH, Wetzlar, Germany). Images were processed, montaged and composed digitally using ImageJ (NIH, Bethesda, MD) and Adobe® Photoshop® CS5.1 software (Adobe Systems Inc., CA, USA). GFP expression in the different layers of the retina was quantitatively evaluated in 7 to 10 retinal vertical sections from each group after subretinal injection. The percentage of the fluorescence in every layer was calculated with ImageJ software (http://imagej.nih.gov/ij/; provided in the public domain by the National Institutes of Health, Bethesda, MD, USA) using a self-developed macro for analysis of acquired image. The same procedure was followed for retinal whole mounts fluorescent measurements after intravitreal injections.

Statistical analysis

Differences between groups were evaluated using a Student's *t* test for unpaired data or a Mann-Whitney *U* test, as appropriate after evaluating normality (Shapiro-Wilks test) and the homogeneity of the variance (Levene test). Data are expressed as mean ± SD. A P value <0.05 was considered statistically significant. Analyses were performed with the IBM SPSS Statistics 22.Ink statistical package.

Results

Physicochemical characterization and stability of niosomes and nioplexes

The physicochemical characteristics of niosomes and nioplexes at the day 0 of the formulation and after 30 days of storage at 4 °C and 25 °C are summarized in Figure 2, *A*. The mean diameter size of niosomes was around 125 nm and remained constant over time and temperature. PDI was lower than 0.20 and zeta potential values increased up to 63.4 mV after 30 days of incubation at 25 °C. In nioplexes, as expected, mean diameter sizes increased when complexing DST20 niosomes with the corresponding DNA material, reaching almost the double of its original diameter (from 123 nm to 239-255 nm), and zeta potential values diminished (from 63.4 mV to 22.7-5.1 mV). As all nioplexes were at the same 2/1 ratio, only slight differences in size were found among nioplexes, ranging from 228 nm to 255 nm. Furthermore, nioplexes maintained proper characteristics for gene therapy applications, with values under 0.3 for PDI and positive zeta potential after 30 days of incubation. Regarding stability of nioplexes, pEGFP 5.5 kb and specially MC-GFP nioplexes kept their size over time independently of the temperature of storage. In contrast, pGFP 3.5 kb nioplexes increased their size specially when stored at 25 °C, which consequently caused a more drastic reduction of its zeta potential value to 5 mV [28].

TEM images (Figure 2, *B*) revealed that DST20 niosomes at day 0 had clear spherical morphology and no aggregations were formed (Figure 2, *B*, *i*); meanwhile a loss of the spherical shape was observed after 30 days of storage (Figure 2, *B*, *ii* and *iii*) and, additionally, a high proportion of aggregates when stored at 25 °C (Figure 2, *B*, *iii*).

The gel retardation assay (Figure 2, *C*) showed that DNA was properly protected from DNase I enzymatic digestion and released after the addition of sodium dodecyl sulfate (SDS) on lanes 3, 6 and 9 corresponding to MC-GFP, pGFP 3.5 kb and pEGFP 5.5 kb nioplexes, respectively. Of note, the signal of these bands was lower in the nioplexes formed with DST20 niosomes stored for 30 days at 4 °C and 25 °C (Figure 2, *C*, *ii* and *iii*, respectively) compared with the ones formed with day 0 DST20 niosomes (Figure 2, *C*, *i*). The absence of bands on lanes 2, 5 and 8 demonstrated that free DNA was completely digested by the DNase I enzyme. In addition, in Figure 2, *C*, *i*, minicircle nioplexes (lane 3) showed better stability under enzymatic digestion, since intensity of lane 6 (pGFP 3.5 kb plasmid) is clearly inferior, and lane 9 (pEGFP 5.5 kb plasmid) shows a long smear. This fact could account for better transfection efficiency of minicircle nioplexes.

A)

Formulation	Z-average size (nm)			PDI			Zeta potential (mV)		
		Day 30			Day 30			Day 30	
	Initial (day 0)	4°C	25°C	Initial (day 0)	4°C	25°C	Initial (day 0)	4°C	25°C
Niosome DST20	123 ± 0	127 ± 1	127 ± 2	0.13 ± 0.01	0.16 ± 0.01	0.19 ± 0.01	51.5 ± 4.5	54.8 ± 5.6	63.4 ± 2.4
Nioplexes:									
DST20:MC-GFP 2.3kb	239 ± 2	234 ± 7	230 ± 1	0.26 ± 0.02	0.25 ± 0.01	0.27 ± 0.01	19.8 ± 3.3	31.8 ± 1.2	22.7 ± 1.4
DST20:pGFP 3.5kb	228 ± 3	250 ± 5	315 ± 7	0.28 ± 0.04	0.24 ± 0.01	0.28 ± 0.03	19.1 ± 1.5	20.3 ± 2.3	5.1 ± 1.1
DST20:pEGFP 5.5kb	255 ± 11	230 ± 3	243 ± 4	0.30 ± 0.06	0.26 ± 0.03	0.25 ± 0.02	14.2 ± 4.5	25.0 ± 1.5	18.4 ± 0.1

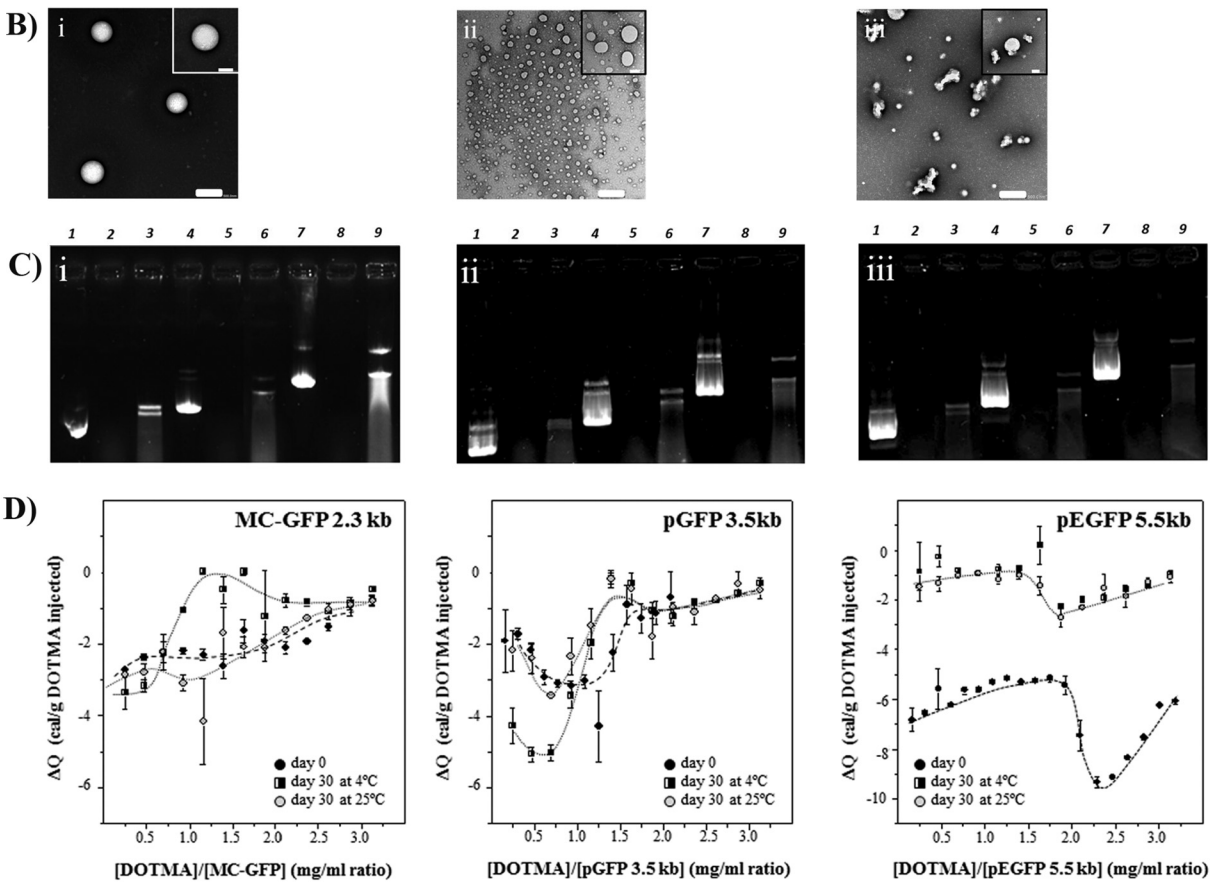

Figure 2. Physicochemical characterization and stability measurements of niosomes and nioplexes.**(A)** Physicochemical characterization of DST20 niosomes at day 0 and at day 30 of storage at 4 °C and 25 °C, and corresponding nioplexes. Each value represents the mean ± SD from three measurements. **(B)** TEM images of DST20 niosomes at day 0 **(i)**, at day 30 of storage at 4 °C **(ii)** and 25 °C **(iii)**. Scale bars: 500 nm (outer images) and 200 nm (inner images). **(C)** Gel retardation assay to analyze the capacity of DST20 niosomes to protect and release the DNA material at day 0 **(i)**, at day 30 of storage at 4 °C **(ii)** and 25 °C **(iii)**. DNase I enzyme and SDS were added in lanes 3, 6 and 9 to evaluate both protection and release in MC-GFP, pGFP 3.5 kb and pEGFP 5.5 kb nioplexes, respectively. As controls, lanes 1, 4 and 7 correspond to control naked MC-GFP, pGFP 3.5 kb and pEGFP 5.5 kb, respectively, and lanes 2, 5 and 8 to those naked DNAs after adding DNase I enzyme, respectively. **(D)** ITC study of DNA titration with DST20 niosomes. Corresponding variation of heat evolved per gram of DOTMA injected *vs.* the ratio of DOTMA/DNA concentrations expressed in mg/ml. Symbols represent the experimental data whereas the discontinuous line illustrate the tendency of the ITC profiles.

ITC data (Figure 2, *D*) represents the heat evolved per injection (normalized per gram of DOTMA injected) as a function of the DOTMA/DNA ratio. At day 0 of niosome formulation (black circles), there was an abrupt change in the titration curves of pGFP 3.5 kb and pEGFP 5.5 kb at values of around 1.25 and 2.0, respectively. As more niosomes were added, the heat released during the injection decreased approaching to zero (Supplementary Figure S1). In addition, a slow process was observed in the raw injection peaks of pGFP 3.5 kb data at ratios 0.9-1.4; meanwhile the formation of MC-GFP and pEGFP 5.5 kb nioplexes proceeded through fast kinetics (Supplementary Figure S2). Remarkably, both the abrupt change in the tendency of the titration profile and the slow process were sensitive to DST20 storage, as evidenced by their shift toward lower DOTMA/DNA ratios when day 30 niosomes were used.

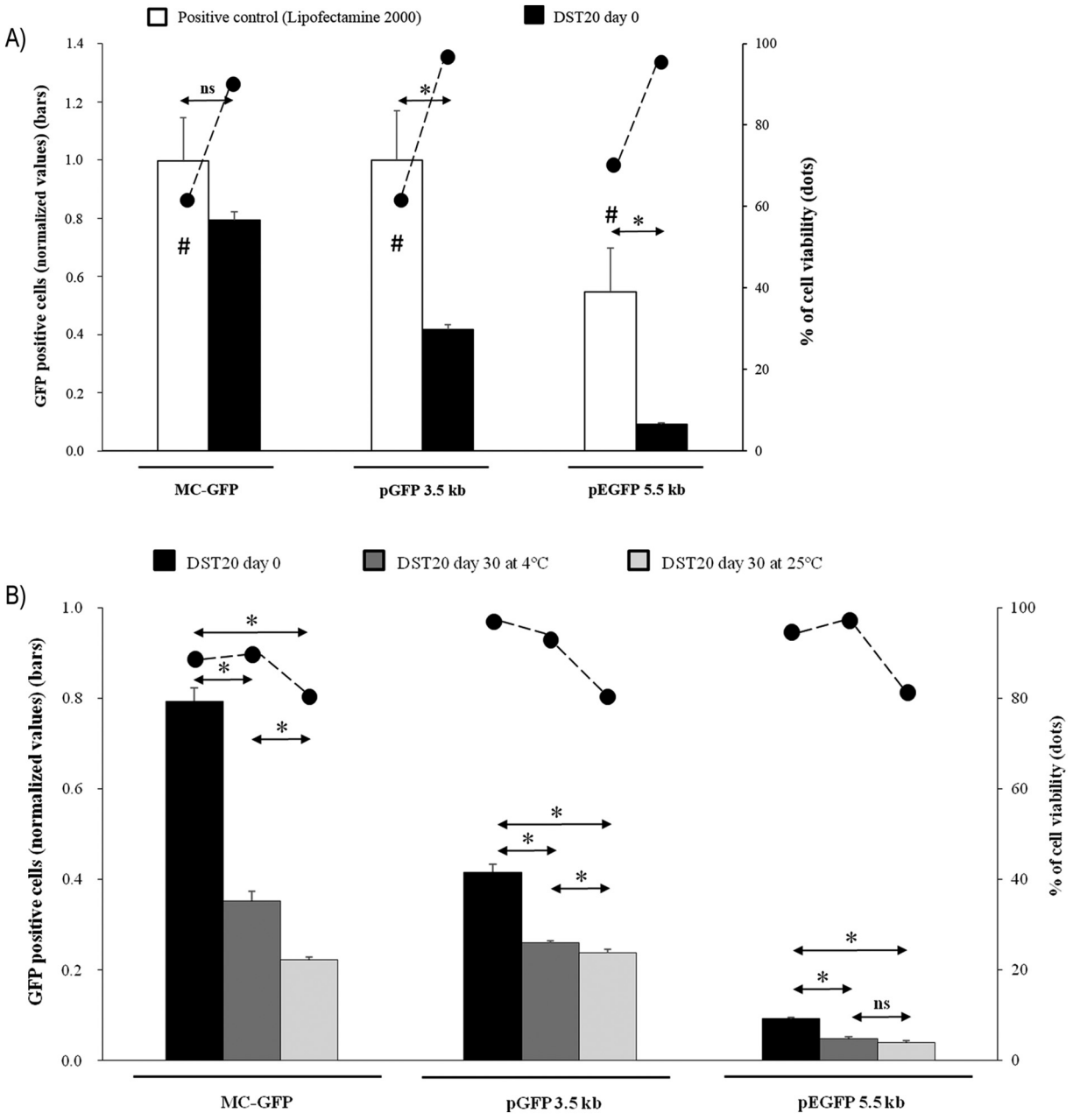

Figure 3. Transfection efficiency of nioplexes and cell viability in ARPE-19 cell line.Flow cytometry evaluation of GFP positive live cells (bars) and viability (dots) after transfection employing **(A)** DST20 niosomes at day 0 and **(B)** after 30 days of storage at 4 °C and 25 °C, bound to either MC-GFP, pGFP 3.5 kb or pEGFP 5.5 kb. Data are presented as mean ± SD, n = 3. *$P < 0.05$ for transfection efficiency groups, #$P < 0.05$ for cell viability relative to its respective Lipofectamine™ 2000; ns means no statistically significant differences.

In vitro studies for transfection efficiency and cell viability over time and storage conditions

The higher rate of transfection observed *in vitro* in ARPE-19 cell line was obtained with MC-GFP and pGFP 3.5 kb Lipofectamine positive controls, with a normalized value of 1 representing a 52% of GFP expression in live cells (Figure 3, *A*, bars). All data were normalized in relation to this value. For DST20 formulation at day 0, there were no significant differences in GFP expression between MC-GFP nioplexes (0.8 ± 0.03) and its positive control (1.0 ± 0.15). In contrast, GFP expression of nioplexes carrying plasmid material was lower than their respective positive controls ($P < 0.05$). In addition, significant differences were found among nioplexes depending on the DNA material complexed to the niosome; thus, DST20 nioplexes containing MC presented higher transfection efficiency than those containing plasmids (MC-GFP: 0.8 ± 0.03; pGFP 3.5 kb: 0.4 ± 0.02; pEGFP 5.5 kb: 0.1 ± 0.01; $P < 0.05$).

Upon DST20 storage for 30 days, transfection efficiency of nioplexes was lower ($P < 0.05$) for every DNA material when compared to that at day 0, reaching the lowest values when stored at 25 °C except for pEGFP 5.5 kb where no differences

were found between 4 °C and 25 °C storage (Figure 3, *B*, bars). Of note, DST20 niosomes stored for 30 days at 4 °C vectoring MC remained exhibiting a higher gene delivery capacity compared with plasmid nioplexes (MC-GFP: 0.35 ± 0.02, pGFP 3.5 kb: 0.26 ± 0.01, pEGFP 5.5 kb: 0.05 ± 0.01; $P < 0.05$). Qualitative analysis of *in vitro* transfection efficiency is reflected in the fluorescence microscopy images shown in Supplementary Figure S3.

Regarding cell viability, DST20 at day 0 nioplexes presented higher rates ($P < 0.05$) of living cells compared with their counterpart positive controls in all cases, reaching values above 90% (Figure 3, *A*, dots). This cell viability remained stable over time when DST20 was stored for 30 days at 4 °C and decreased to 80% values when stored at 25 °C (Figure 3, *B*, dots).

Immunofluorescence analysis of GFP expression in embrionary rat retinal primary cells

Transfection assays showed GFP expression in retinal primary cells exposed to DST20 at day 0 of nioplexes for every DNA material (Figure 4). Fluorescence signal emitted by MC-GFP, pGFP 3.5 kb and pEGFP 5.5 kb plasmids vectored by DTS20 niosomes was observed in cells that were negative to MAP2 staining. In addition, such transfected cells showed glial cell morphology (Figure 4, *A-C*). Accordingly, glial morphology like cells too showed transgene expression when vectored by their counterpart positive control (Figure 4, *D-F*, respectively). More confocal image pictures of rat primary retinal cell cultures transfected with complexes that corroborate the results can be found in the supplementary data, as Supplementary Figure S4.

Analysis of GFP expression in vivo

GFP expression was found in rat retinas 72 h upon IV and SR administration of DST20 nioplexes vectoring any of the three DNA materials (Figures 5 and 6), whereas no fluorescence signal was detected in control retinas (data not shown).

The analysis of whole-mount preparations after IV administration of DST20 nioplexes showed in all cases GFP expression in the ganglion cell layer (GCL) (Figure 5). SR administration of DST20 nioplexes vectoring either MC-GFP, pGFP 3.5 kb or pEGFP 5.5 kb (Figure 6, *A-C*, respectively) was analyzed in sagittal retinal sections, showing GFP expression located in different retinal cell layers. Some fluorescence signal was located in the inner nuclear layer (INL), especially for MC which showed also GFP expression in the ganglion cell layer (GCL). In all cases, GFP signal was mainly observed in the outer segments (OS) of the photoreceptors and, importantly, at the retinal pigment epithelium level (RPE). Qualitative analysis after both IV and SR injections showed that MC-GFP nioplexes resulted in the higher rate of GFP expression, diminishing progressively with pGFP 3.5 kb and pEGFP 5.5 kb nioplexes.

Discussion

The main findings of this study are the following: (1) DST20 niosomes is a non-viral vector able to protect genetic material and release it with controlled kinetics; (2) the capacity of niosomes to protect and interact with DNA material is affected over time and temperature of storage; (3) DST20 niosomes

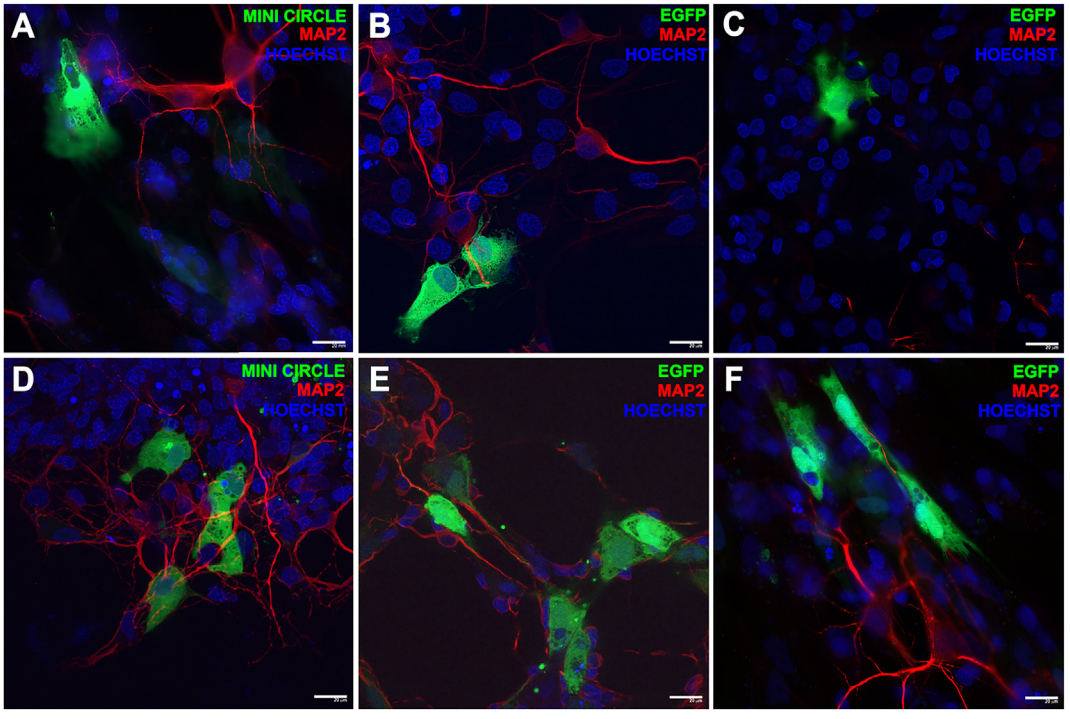

Figure 4. GFP expression in embrionary rat retinal primary cells.Fluorescence immunocytochemistry showing GFP positive signal after transfection with DST20 nioplexes, carrying either **(A)** MC-GFP, **(B)** pGFP 3.5 kb or **(C)** pEGFP 5.5 kb. **(D-F)** Images of their counterpart positive controls exposed to Lipofectamine™ 2000. Cell nuclei were counterstained with Hoechst 33342 (pseudocolored blue) and neuronal dendrites with MAP2 (red color). Scale bars: 20 μm.

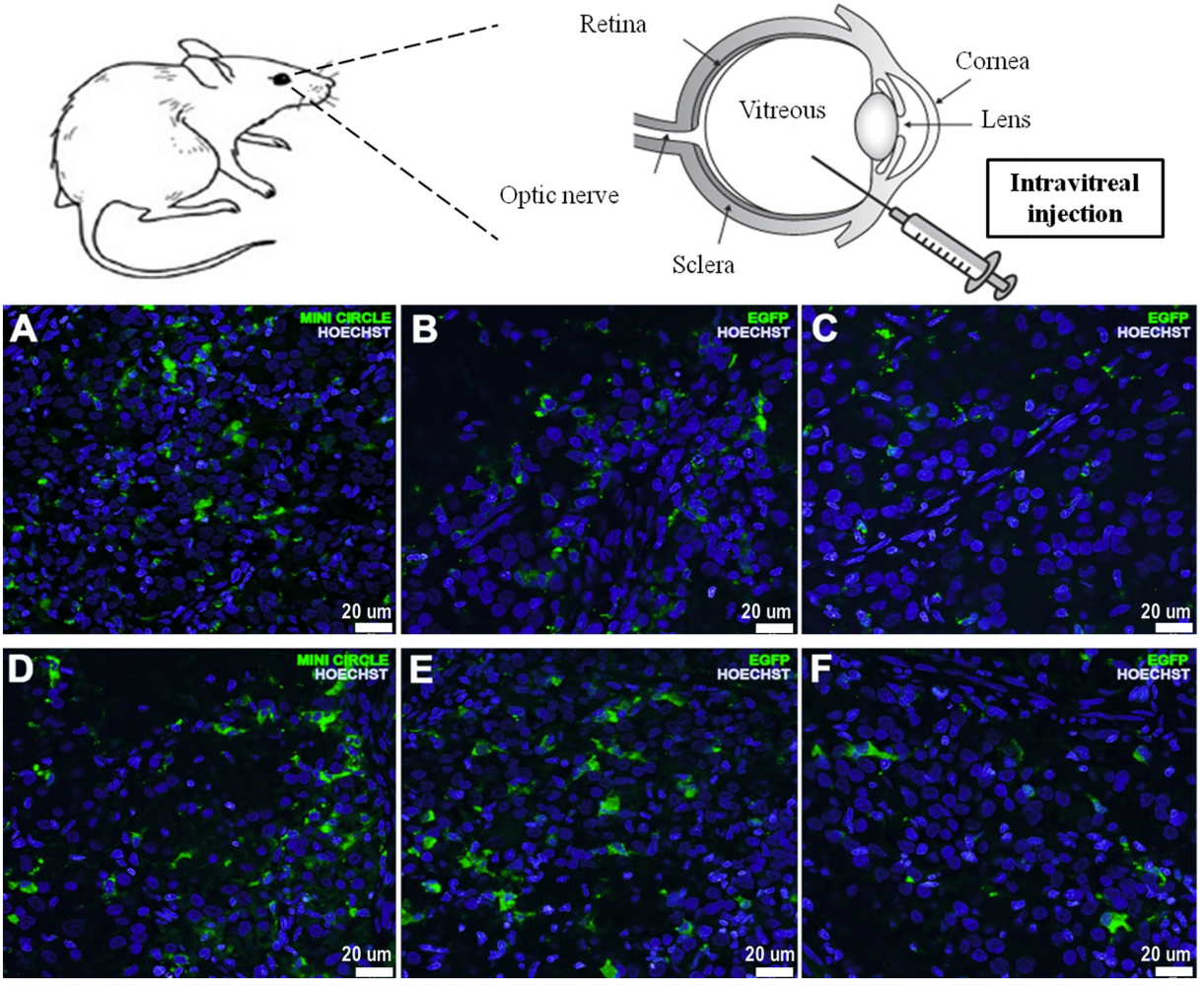

Figure 5. *In vivo* expression of GFP after intravitreal injection of nioplexes.Fluorescence immunohistochemistry in a whole-mounted vitreous side-up retinal section showing GFP positive signal located in the ganglion cell layer after intravitreal administration of DST20 nioplexes carrying either **(A)** MC-GFP, **(B)** pGFP 3.5 kb or **(C)** pEGFP 5.5 kb. **(D-F)** Images of their counterpart positive controls. Cell nuclei were counterstained with Hoechst 33342 (pseudocolored blue). Scale bars: 20 μm.

complexed with different genetic material, varying in terms of size and composition, present similar size and zeta potential but have different transfection efficiencies *in vitro*; meanwhile cell viability is not affected; (4) DST20 nioplexes containing MC-DNA present higher transfection efficiency than those containing plasmids in *in vitro* assays, even after DST20 storage for 30 days; and (5) DST20 nioplexes are able to transfer the genetic material not only in *ex vivo* primary retinal cell cultures but also after *in vivo* injection in rat retinas regardless the *via* of administration, being those carrying MC-DNA the ones that present the higher rate of GFP signal. Therefore, DST20 niosomes vectoring MC technology seems to be an efficient and safe therapeutic tool for retinal disorders, overcoming the existing translational barrier of non-viral vectors complexed with plasmids due to their poor transfection efficiency.

DST20 niosomes presented appropriate spherical morphology and size for gene therapy purposes, 123 nm, with low PDI and positive zeta potential pointing out not only a good homogeneity and stability of the suspensions, but also an easy interaction with the negatively charged phosphate groups of the DNA material to form nioplexes, respectively [29–31]. It is worth mentioning that differences in the reported size of niosomes between dynamic light scattering and TEM techniques could be explained by the sample processing and treatment performed for both analyses [32]. As expected, complexation of DST20 niosomes with the corresponding DNA almost doubled its original diameter and zeta potential values diminished due to the partial neutralization of the positive amine groups of niosomes by the DNA phosphate groups.

The features observed regarding size, zeta potential and transfection efficiency when complexing niosomes to the three genetic materials, are in accordance with previous studies which confirm that the DNA size bound to niosomes does not affect such physicochemical properties of nioplexes [33] but have different transfection efficiencies *in vitro* [34]. The explanation for the differences observed in transfection efficiencies might reside in two main factors. On the one hand, the magnitude of the increment in the particle-size of nioplexes with respect to the

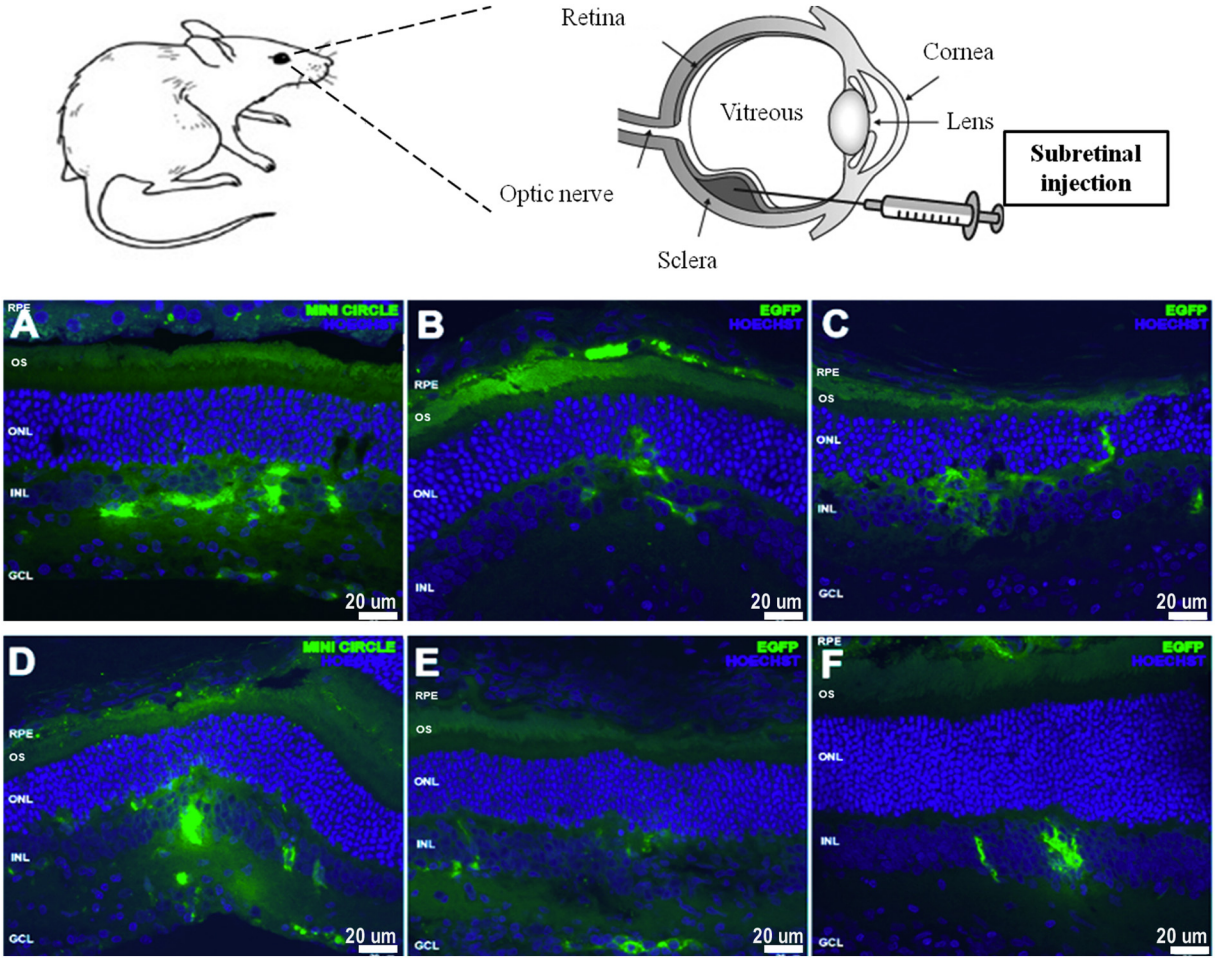

Figure 6. *In vivo* expression of GFP after subretinal injection of nioplexes.Confocal fluorescence micrographs of retinal cross sections showing GFP signal after subretinal administration of DST20 nioplexes carrying either **(A)** MC-GFP, **(B)** pGFP 3.5 kb or **(C)** pEGFP 5.5 kb. **(D-F)** Images of their counterpart positive controls. RPE (retinal pigment epithelium), OS (outer segments), ONL (outer nuclear layer), INL (inner nuclear layer), GCL (ganglion cell layer). Cell nuclei were counterstained with Hoechst 33342 (pseudocolored blue). Scale bars: 20 μm.

niosomes seems to rule out the possibility that the second phase seen in the ITC titration curves might be due to the binding of more niosomes onto DNA-coated nioplexes. Thus, niosome-DNA binding events occurring at higher ratios than 2/1 would probably involve the reorganization of the previously bound genetic material, which would lead to a reduction in the number of DNA molecules bound per niosome and to the preferential occupation of the most favorable binding sites on the niosome surface. This could also affect the ability of the nioplexes to interact with the cell surface and, consequently, their transfection capacity. On the other hand, this study was developed with a constant DNA quantity of 1.25 μg per condition but it has to be taken into account that DNA length – and therefore weight and molarity – differs between the three genetic materials under study, which consequently affects the number of DNA molecules bound to each niosome. This fact can be observed in the ITC assay where different calorimetry curves were obtained depending on the genetic material complexed to the DST20 formulation. Hence, niosomes would be incorporating more MC molecules than plasmids ones, which means a higher rate of expression cassettes per niosome, increasing the probability of efficient gene delivery into the cell and finally a higher transgene expression [25,34].

The differences found in GFP expression upon the storage of niosomes could be explained not by a single cause but by several cumulative reasons. In fact, effective gene delivery is affected by size range and zeta potential but many other relevant parameters such as a correct vector morphology and DNA binding affinity may impact on this effectiveness [35]. In this regard, TEM images showed a loss of the spherical shape of niosomes and even the formation of some aggregates after 30 days of storage, which in turn would difficult interactions with the DNA material. Actually, gel retardation and ITC assays confirm this reduction of DNA complexation capacity of niosomes over time. In agarose gels, the lower signal of bands corresponding to DNA protection and release after storage denoted a reduction of these capacities. Accordingly, ITC data would be indicative that the molecular features of the DST20-based nioplexes formed at 2.0 ratio (equivalent to DOTMA/DNA ratio 2/1) could depend on the previous history of the niosomes, explaining the differences mentioned before, such as the physicochemical features, the morphology of niosomes and their ability to protect and release

the DNA. Even though DST20 niosomes stored for 30 days at 4 °C vectoring MC remained exhibiting a higher gene delivery capacity compared with plasmid nioplexes, additional efforts are required in order to achieve more stable formulations by either performing better characterization methods or by introducing modifications into formulations themselves. Regarding cell viability, the slightly lower values obtained with DST20/MC (2.3 kb) nioplexes compared to both DST20/ pGFP(3.5 kb) and DST20 pEGFP (5.5 kb) at day 0, could be explained by the higher transfection efficiencies obtained with this formulation, since the transfection process itself can cause cellular toxicity. Anyway, all DST20 nioplexes vectoring the three different genetic materials exhibited excellent cell viability values around 90% at day 0, significantly higher than those obtained with positive control Lipofectamine™ 2000 (around 60%), indicating that they were well tolerated by cells. In embrionary rat retinal primary cell cultures, DST20 nioplexes showed clear transgene expression with high cell viability in all conditions. Such transfected cells were negative to MAP2 staining and had glial cells morphology. This kind of cells could have been transfected due to their higher phagocytic capacity.

Since IV and SR routes are considered the most clinically viable options to deliver efficiently the genetic material to the back of the eye [36], nioplexes were injected at these levels *in vivo*. In both cases, we did not observe any sign of toxicity or inflammation of the eye fundus upon administrations (data not shown). IV administration of DST20 nioplexes showed GFP expression in the GCL, in accordance with previous works employing non-viral vectors [17,18]. Effective gene transfer at this level could be clinically relevant for treatment of devastating inherited retinal disorders such as glaucoma, which is considered the first cause of blindness worldwide [37]. After injection of those nioplexes at SR level, transgene expression diffused to the inner nuclear layer (INL) and, importantly, was localized close to the injection site in the retinal pigment epithelium (RPE). For therapeutic clinical practice, gene delivery reaching the outer layers of the retina is deeply desirable since many inherited retinal disorders with no curative treatment to date, such as retinitis pigmentosa, Stagardt's disease or Leber's congenital amaurosis, are associated with more than 200 mutations of genes expressed at the photoreceptors and RPE level [4]. Qualitative analysis after both IV and SR injections showed a higher transgene expression the smaller the DNA was, pointing out that DST20 non-viral vector combined with MC-DNA offers a potential tool for retinal degenerative and inherited diseases. This qualitative analysis was further confirmed by the quantitative analysis (Supplementary Figure S5). In addition, it has been reported that MC technology offers not only a higher but also a sustained gene expression over time, offering key benefits for clinical translation [25,34]. Although GFP expression was also observed employing Lipofectamine™ 2000, it has been shown that such formulation is not suitable for *in vivo* experiments due to its high toxicity mainly accused into photoreceptor cells even at low concentrations [38]. In fact, our *in vitro* experiments clearly showed the toxicity of Lipofectamine™ 2000 in retinal cells. Finally, the high transfection efficiency achieved with DST20/MC nioplexes at the low 2/1 ratio is noteworthy since it allows a higher gene content at small volumes of injection for clinical applications, where the volume to be injected represents an important handicap, and reduces cellular toxicity associated to cationic lipids [39]. Furthermore, the lack of unmethylated CpG content in MC-DNA technology provides additional reduced immunogenic responses, reinforcing DST20/MC complexes as a potential efficient and safe tool for translational retinal gene therapy applications.

Appendix A. Supplementary data

Supplementary data to this article can be found online at https://doi.org/10.1016/j.nano.2018.12.018.

References

1. Francis PJ. Genetics of inherited retinal disease. *JR Soc Med* 2006;**99**:189-91.
2. Fritsche LG, Igl W, Bailey JN, Grassmann F, Sengupta S, Bragg-Gresham JL, et al. A large genome-wide association study of age-related macular degeneration highlights contributions of rare and common variants. *Nat Genet* 2016;**48**:134-43.
3. McClements ME, MacLaren RE. Gene therapy for retinal disease. *Transl Res* 2013;**161**:241-54.
4. Lipinski DM, Thake M, MacLaren RE. Clinical applications of retinal gene therapy. *Prog Retin Eye Res* 2013;**32**:22-47.
5. Ramamoorth M, Narvekar A. Non viral vectors in gene therapy- an overview. *J Clin Diagn Res* 2015;**9**:GE01-6.
6. Mingozzi F, High KA. Therapeutic in vivo gene transfer for genetic disease using AAV: progress and challenges. *Nat Rev Genet* 2011;**12**:341-55.
7. Provost N, Le Meur G, Weber M, Mendes-Madeira A, Podevin G, Cherel Y, et al. Biodistribution of rAAV vectors following intraocular administration: evidence for the presence and persistence of vector DNA in the optic nerve and in the brain. *Mol Ther* 2005;**11**:275-83.
8. Mingozzi F, High KA. Immune responses to AAV vectors: overcoming barriers to successful gene therapy. *Blood* 2013;**122**:23-36.
9. Keles E, Song Y, Du D, Dong WJ, Lin Y. Recent progress in nanomaterials for gene delivery applications. *Biomater Sci* 2016;**4**:1291-309.
10. Rajera R, Nagpal K, Singh SK, Mishra DN. Niosomes: a controlled and novel drug delivery system. *Biol Pharm Bull* 2011;**34**:945-53.
11. Choi WJ, Kim JK, Choi SH, Park JS, Ahn WS, Kim CK. Low toxicity of cationic lipid-based emulsion for gene transfer. *Biomaterials* 2004;**25**:5893-903.
12. Karmali PP, Chaudhuri A. Cationic liposomes as non-viral carriers of gene medicines: resolved issues, open questions, and future promises. *Med Res Rev* 2007;**27**:696-722.
13. Dabkowska AP, Barlow DJ, Campbell RA, Hughes AV, Quinn PJ, Lawrence MJ. Effect of helper lipids on the interaction of DNA with cationic lipid monolayers studied by specular neutron reflection. *Biomacromolecules* 2012;**13**:2391-401.
14. Ojeda E, Puras G, Agirre M, Zarate J, Grijalvo S, Eritja R, et al. The role of helper lipids in the intracellular disposition and transfection efficiency of niosome formulations for gene delivery to retinal pigment epithelial cells. *Int J Pharm* 2016;**503**:115-26.
15. Taymouri S, Varshosaz J. Effect of different types of surfactants on the physical properties and stability of carvedilol nano-niosomes. *Adv Biomed Res* 2016;**5**:48, https://doi.org/10.4103/2277-9175.178781 (eCollection 2016).
16. Puras G, Martinez-Navarrete G, Mashal M, Zarate J, Agirre M, Ojeda E, et al. Protamine/DNA/Niosome Ternary Nonviral Vectors for Gene Delivery to the Retina: The Role of Protamine. *Mol Pharm* 2015;**12**:3658-71.

17. Mashal M, Attia N, Puras G, Martinez-Navarrete G, Fernandez E, Pedraz JL. Retinal gene delivery enhancement by lycopene incorporation into cationic niosomes based on DOTMA and polysorbate 60. *J Control Release* 2017;**254**:55-64.
18. Ojeda E, Puras G, Agirre M, Zarate J, Grijalvo S, Eritja R, et al. The role of helper lipids in the intracellular disposition and transfection efficiency of niosome formulations for gene delivery to retinal pigment epithelial cells. *Int J Pharm* 2016;**503**:115-26.
19. Puras G, Mashal M, Zarate J, Agirre M, Ojeda E, Grijalvo S, et al. A novel cationic niosome formulation for gene delivery to the retina. *J Control Release* 2014;**174**:27-36.
20. Hardee CL, Arevalo-Soliz LM, Hornstein BD, Zechiedrich L. Advances in Non-Viral DNA Vectors for Gene Therapy. *Genes (Basel)* 2017;**8**, https://doi.org/10.3390/genes8020065.
21. Gracey Maniar LE, Maniar JM, Chen ZY, Lu J, Fire AZ, Kay MA. Minicircle DNA vectors achieve sustained expression reflected by active chromatin and transcriptional level. *Mol Ther* 2013;**21**:131-8.
22. Ahmad-Nejad P, Hacker H, Rutz M, Bauer S, Vabulas RM, Wagner H. Bacterial CpG-DNA and lipopolysaccharides activate Toll-like receptors at distinct cellular compartments. *Eur J Immunol* 2002;**32**:1958-68.
23. Tidd N, Michelsen J, Hilbert B, Quinn JC. Minicircle Mediated Gene Delivery to Canine and Equine Mesenchymal Stem Cells. *Int J Mol Sci* 2017;**18**, https://doi.org/10.3390/ijms18040819.
24. Gaspar V, de Melo-Diogo D, Costa E, Moreira A, Queiroz J, Pichon C, et al. Minicircle DNA vectors for gene therapy: advances and applications. *Expert OpinBiolTher* 2015;**15**:353-79.
25. Fernandes AR, Chari DM. Part I: Minicircle vector technology limits DNA size restrictions on ex vivo gene delivery using nanoparticle vectors: Overcoming a translational barrier in neural stem cell therapy. *J Control Release* 2016;**238**:289-99.
26. Liu N, Wang BJ, Broughton KM, Alvarez R, Siddiqi S, Loaiza R, et al. PIM1-minicircle as a therapeutic treatment for myocardial infarction. *PLoS One* 2017;**12**e0173963.
27. Villate-Beitia I, Puras G, Soto-Sanchez C, Agirre M, Ojeda E, Zarate J, et al. Non-viral vectors based on magnetoplexes, lipoplexes and polyplexes for VEGF gene delivery into central nervous system cells. *Int J Pharm* 2017;**521**:130-40.
28. Wissing SA, Kayser O, Muller RH. Solid lipid nanoparticles for parenteral drug delivery. *Adv Drug Deliv Rev* 2004;**56**:1257-72.
29. Gratton SE, Ropp PA, Pohlhaus PD, Luft JC, Madden VJ, Napier ME, et al. The effect of particle design on cellular internalization pathways. *Proc Natl Acad Sci USA* 2008;**105**:11613-8.
30. Jacobs C, Kayser O, Muller RH. Nanosuspensions as a new approach for the formulation for the poorly soluble drug tarazepide. *Int J Pharm* 2000;**196**:161-4.
31. Hosseinkhani H, Tabata Y. Self assembly of DNA nanoparticles with polycations for the delivery of genetic materials into cells. *J Nanosci Nanotechnol* 2006;**6**:2320-8.
32. Ojeda E, Puras G, Agirre M, Zarate J, Grijalvo S, Pons R, et al. Niosomes based on synthetic cationic lipids for gene delivery: the influence of polar head-groups on the transfection efficiency in HEK-293, ARPE-19 and MSC-D1 cells. *Org Bio mol Chem* 2015;**13**:1068-81.
33. Kreiss Patrick, et al. Plasmid DNA size does not affect the physicochemical properties of lipoplexes but modulates gene transfer efficiency. *Nucleic Acids Res* 1999;**27**:3792-8.
34. Klausner EA, Zhang Z, Wong SP, Chapman RL, Volin MV, Harbottle RP. Corneal gene delivery: chitosan oligomer as a carrier of CpG rich, CpG free or S/MAR plasmid DNA. *J Gene Med* 2012;**14**:100-8.
35. Rezvani Amin Z, Rahimizadeh M, Eshghi H, Dehshahri A, Ramezani M. The effect of cationic charge density change on transfection efficiency of polyethylenimine. *Iran J Basic Med Sci* 2013;**16**:150-6.
36. Conley SM, Naash MI. Nanoparticles for retinal gene therapy. *Prog Retin Eye Res* 2010;**29**:376-97.
37. Almasieh M, Wilson AM, Morquette B, Cueva Vargas JL, Di Polo A. The molecular basis of retinal ganglion cell death in glaucoma. *Prog Retin Eye Res* 2012;**31**:152-81.
38. Kachi S, Oshima Y, Esumi N, Kachi M, Rogers B, Zack DJ, et al. Nonviral ocular gene transfer. *Gene Ther* 2005;**12**:843-51.
39. Shao XR, Wei XQ, Song X, Hao LY, Cai XX, Zhang ZR, et al. Independent effect of polymeric nanoparticle zeta potential/surface charge, on their cytotoxicity and affinity to cells. *Cell Prolif* 2015;**48**:465-74.